



Influence of pulse plating parameters on the synthesis and preferred orientation of nanocrystalline zinc from zinc sulfate electrolytes

K.M. Youssef^{a,*}, C.C. Koch^a, P.S. Fedkiw^b

^a Department of Materials Science and Engineering, North Carolina State University, Raleigh, NC 27695-7907, USA

^b Department of Chemical and Biomolecular Engineering, North Carolina State University, Raleigh, NC 27695-7905, USA

ARTICLE INFO

Article history:

Received 13 May 2008

Received in revised form 1 July 2008

Accepted 2 July 2008

Available online 29 July 2008

Keywords:

Pulse electrodeposition

Nanocrystalline

Zinc

Preferred orientation

ABSTRACT

The influence of pulse electrodeposition parameters (current on-time T_{on} , current off-time T_{off} , and pulse current density J_p) was investigated on the surface morphology and grain size of zinc electrodeposited from a sulfate bath containing polyacrylamide and thiourea additives. The grain size and surface morphology of zinc deposits were studied by field emission scanning electron microscopy (FESEM) and atomic force microscopy (AFM), and the preferred orientation of the deposits was studied by X-ray diffraction. At constant current off-time and pulse current density, the grain size decreased asymptotically with increasing current on-time. In contrast, increase in the current off-time at constant current on-time and pulse current density resulted in grain growth. A progressive decrease of the grain size was observed with increasing pulse current density at constant current on-time and off-time. Nanocrystalline zinc with an average grain size of 38 nm was obtained at a pulse current density of 1200 mA/cm². The crystallographic orientations developed were correlated with the change in the cathodic overpotential, the angle between the preferred oriented plane and the lowest energy of formation plane (0002), and the pulse electrodeposition parameters.

Published by Elsevier Ltd.

1. Introduction

Since the introduction of nanocrystalline materials by Gleiter [1], a search for new preparation methods to produce these materials occupies scientists worldwide. Pulse electrodeposition is a versatile method that was proven recently to produce nanocrystalline materials [2–5]. Pulse plating parameters (current on-time (T_{on}), current off-time (T_{off}), and pulse current density (J_p)) play a major role in controlling the electrocrystallization process, and hence the microstructure and properties of the deposits. Unfortunately, the results obtained by different researchers for a particular electrolyte–electrode system are not comparable and, in many cases, are contradictory, which may be attributed to: (1) the complexity of the electrodeposition process; (2) the large number of experimental variables involved in electrodeposition; (3) the lack of standardized procedure in investigating the effect of a certain pulse parameter [6]. For instance, Puipe and Ibl [7] studied the surface morphology of cadmium, gold, and copper pulse-plated at constant pulse current density and current on-time, but with different values of current off-times. It was found that longer off-

times lead to grain refinement for cadmium, but to grain growth for gold and copper. Pulse electrodeposition results of zinc, which is a well-known coating to protect steel against corrosion, also show some contradictions. Paatsch [8] has shown that grain size of zinc deposits can be minimized by short current on-time in the range from 0.1 to 1 ms in a zinc chloride-based electrolyte. However, we [3] observed grain-size refinement of zinc deposits with increasing current on-time in the range of 0.1–5 ms.

Texture development is observed in many electrodeposits because grains of a particular orientation grow preferentially. A number of researchers have hypothesized on causes for the textural phenomenon [9,10]. However, most explanations are correlated to either the system being studied and/or a specific material property (e.g., magnetic). It has also been reported that zinc electrodeposits produced from zinc chloride electrolyte with additives (animal glue) under direct current plating conditions develop a sequence of preferred orientations in the order $(10\bar{1}3)$, $(10\bar{1}2)$, $(11\bar{2}4)$, $(11\bar{2}2)$, $(10\bar{1}1)$, $(11\bar{2}0)$ [11]. The authors attributed this sequence of preferred orientations to the increase of overpotential with increasing direct current density. Although most textural developments observed in zinc and other deposits (produced by direct current plating) are linked with the value of cathodic overpotential [10,11], the pulse plating parameters might have some contribution to the textures formed during pulse electrodeposition.

* Corresponding author. Tel.: +1 919 515 7217; fax: +1 919 515 7724.
E-mail address: khaled.youssef@ncsu.edu (K.M. Youssef).

Table 1
Composition of the zinc sulfate-plating bath

ZnSO ₄ ·7H ₂ O	0.52 M
(NH ₄) ₂ SO ₄	0.15 M
Polyacrylamide (MW = 200,000)	0.7 g/l
Thiourea	0.05 g/l
pH	4
Temperature	23 ± 1 °C

The main goal of the present study is to optimize the pulse plating parameters (T_{on} , T_{off} , and J_p) in order to produce nanocrystalline zinc deposits from a zinc sulfate-based electrolyte. In addition to the effect of cathodic overpotential, we describe how variations of the pulse parameters offer a possible means to control the preferred orientation evolved.

2. Experimental

Zinc deposits, 12.5 μm in thickness, were deposited onto a cold-rolled, low-carbon steel disk (0.317 cm²) from a bath containing ZnSO₄·7H₂O, (NH₄)₂SO₄ (Fisher Scientific), polyacrylamide (Fisher Scientific), and thiourea (Aldrich) at pH and temperature of 4 and 23 ± 1 °C, respectively. A 4-cm², high-purity (99.99%) zinc sheet (Aldrich) was used as a soluble anode. Pulse electrodeposition of zinc deposits was carried out using a rotating disk electrode in a 250-mL cell. At least two replicates were used for every measurement. The electrolyte composition used throughout this study is shown in Table 1. Concentration of polyacrylamide and thiourea were selected according to results described in [3]. The range of pulse electrodeposition parameters (T_{on} , T_{off} , and J_p) investigated in this study to produce nanocrystalline zinc is shown in Table 2. Each parameter is varied while the other two are held constant.

A PowerLab/4s (Chart version 4.1.2, ADInstruments) was used to generate the current waveforms and record both the current and the potential between the cathode and the saturated calomel reference electrode (SCE). A PAR 173 potentiostat/galvanostat was used to supply the current. The uncompensated ohmic potential drop (IR_u) between the working and reference electrodes was cal-

Table 2
Range of pulse electrodeposition parameters used in this study

Parameter	Range
Current on-time (ms)	1–7
Current off-time (ms)	9–50
Pulse current density (mA/cm ²)	400–1200
Duty cycle (%)	2–44

culated from the measured uncompensated ohmic resistance (R_u). The ohmically corrected overpotential was determined by subtracting the open-circuit potential from the ohmically corrected working electrode potential. In the window of values used in this study for T_{on} and T_{off} , the potential was essentially constant during the respective times.

The microstructure of zinc deposits was examined by a field emission scanning electron microscope (JEOL 6400F), and atomic force microscopy (AFM) was used to examine the grain size and surface morphology of the smallest nano-grained zinc deposits. X-ray diffraction analysis was carried out by using a Rigaku diffractometer (model D/MAX A series X-ray) with Cu K α radiation ($\lambda = 0.15405$ nm). Preferred orientation of the zinc electrodeposits was calculated from the X-ray data according to the method proposed by Berube and Esperance [12].

3. Results and discussion

3.1. Current on-time

The influence of pulse duration T_{on} on the morphology and grain size of zinc deposits, with constant pulse current density and current off-time, is illustrated in Figs. 1 and 2. These micrographs show that an increase in T_{on} results in a decrease in grain size of zinc deposits. Zinc platelets with an average grain size of 195 nm are formed at $T_{on} = 1$ ms (Figs. 1a and 2), while increasing T_{on} to 3 ms (Fig. 1b) results in disappearance of the sharp edges of zinc platelets with a slight reduction of the average grain size to 157 nm (Fig. 2). Further increase of current on-time to 5 and 7 ms dras-

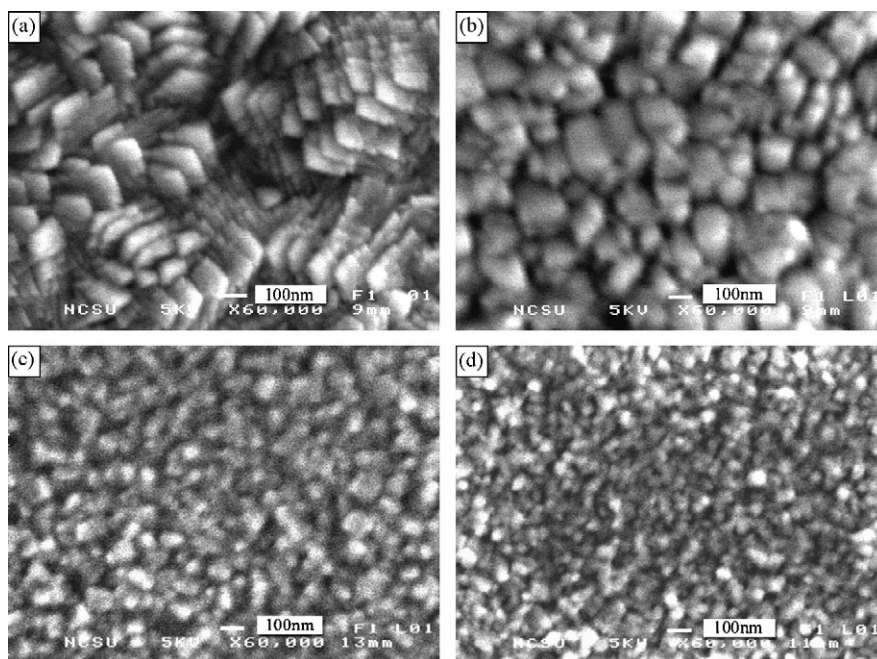


Fig. 1. FESEM micrographs of the surface morphology of zinc deposits obtained at $T_{off} = 9$ ms, $J_p = 800$ mA/cm² and different current on-times: (a) 1 ms, (b) 3 ms, (c) 5 ms, and (d) 7 ms.

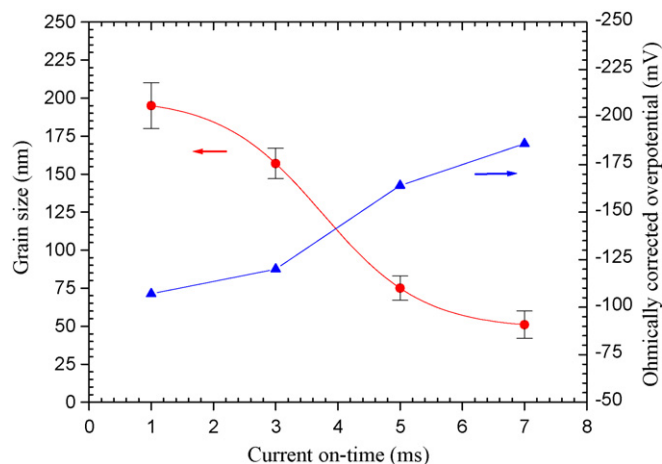


Fig. 2. Variation of grain size and ohmically corrected overpotential of zinc deposits with current on-time at $T_{\text{off}} = 9$ ms, and $J_p = 800$ mA/cm².

tically reduces the average grain size of zinc deposits to 75 and 51 nm, respectively (Figs. 1c and d and 2). The trend of decreasing grain size with increasing current on-time can best be explained by an increased number of nucleation sites caused by the higher overpotential at longer current on-times. The variation of the cathodic overpotentials at the studied T_{on} values is shown in Fig. 2, which reveals that the overpotential increases (negatively) with increasing current on-time and nanocrystalline zinc deposit (51 nm) was formed at the highest overpotential (–186 mV). The same behavior of increasing overpotential with current on-time was also found during zinc deposition from a chloride-based electrolyte but at lower overpotential [3]. Other researchers have reported a decrease in grain size of gold [13] and palladium [14] electrodeposits with increasing current on-time, which they attributed to an increased nucleation rate resulting from the higher overpotential.

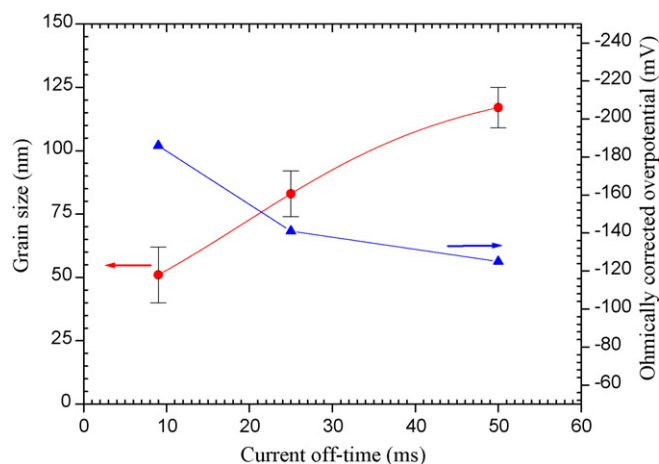


Fig. 4. Variation of grain size and ohmically corrected overpotential of zinc deposits with current off-time at $T_{\text{on}} = 7$ ms, and $J_p = 800$ mA/cm².

3.2. Current off-time

FESEM micrographs showing the effect of current off-time on the grain size and surface morphology of zinc deposits are illustrated in Fig. 3. The current off-time was varied from 9 to 50 ms at the “optimized” T_{on} value (7 ms) and pulse current density of 800 mA/cm². Throughout the rest of the paper, “optimized” parameter means the value that yields deposits with the smallest grain size. The average grain size of the deposits increased gradually from 51 to 117 nm with increasing current off-time from 9 to 50 ms, respectively (Figs. 3 and 4). The formation of large grains at longer off-times can be plausibly explained by desorption of some species (most likely additives and/or hydrogen) during the longer off-times which activates the growth centers and results in grain growth. Also zinc adatoms at longer off-times have sufficient time

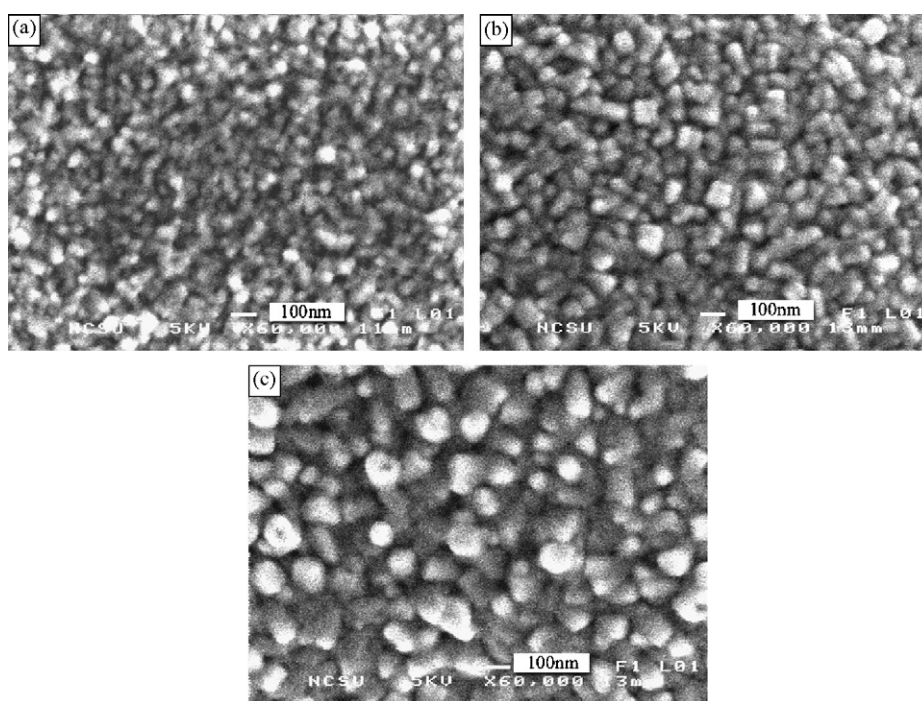


Fig. 3. FESEM micrographs of the surface morphology of zinc deposits obtained at $T_{\text{on}} = 7$ ms, $J_p = 800$ mA/cm² and different current off-times (a) 9 ms, (b) 25 ms, and (c) 50 ms.

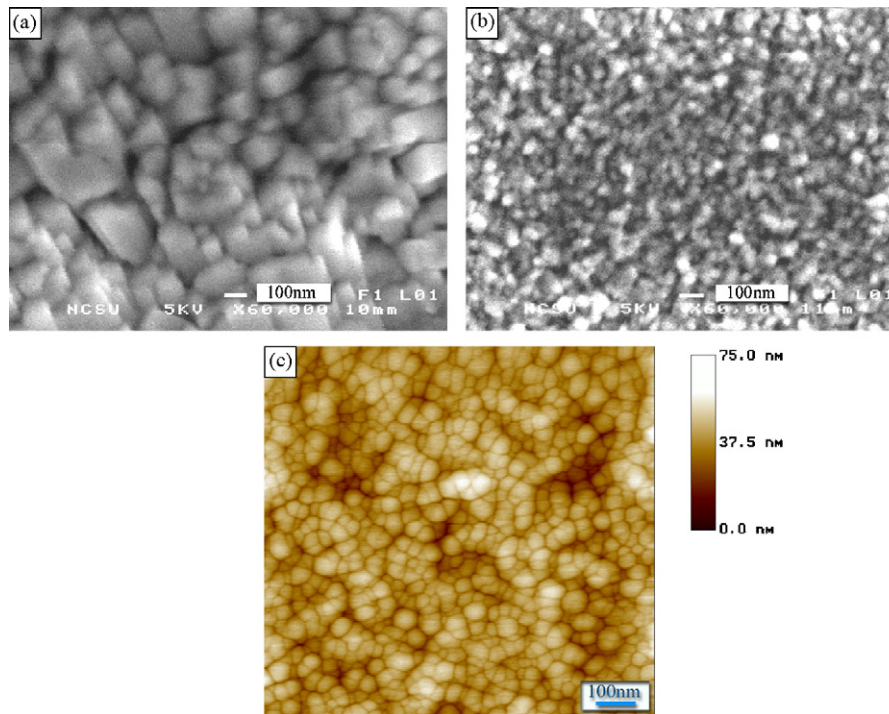


Fig. 5. FESEM micrographs and AFM image of the surface morphology of zinc deposits obtained at $T_{\text{on}} = 7$ ms, $T_{\text{off}} = 9$ ms, and different pulse current densities (a) 400, (b) 800, and (c) 1200 mA/cm².

to migrate over the crystal surface and enhance the grain growth-process. Puippe [15] obtained grain coarsening during pulse plating of copper and gold deposits at long off-times while the current on-time and pulse current density were held constant. They explained this trend in terms of a recrystallization process and argued that coarse grains are thermodynamically more stable and longer off-time provides enough time for the system to stabilize and therefore grain growth takes place. Fig. 4 shows the variation of grain size and ohmically corrected overpotential of zinc deposits with current off-time. The cathodic overpotential decreases gradually with increasing current off-time; a result that may also be plausibly used to explain the grain coarsening at longer off-times.

3.3. Pulse current density

Figs. 5 and 6 show the effect of pulse current density on the microstructure and grain size of zinc deposits obtained at 400, 800, and 1200 mA/cm². The current on-time and off-time were kept at the optimized values 7 and 9 ms, respectively. An average zinc grain size of 300 nm was obtained at a pulse current density of 400 mA/cm² (Figs. 5a and 6). Increasing the pulse current density to 800 mA/cm² (Figs. 5b and 6) results in a progressive decrease in the grain size of the deposits down to 51 nm. The smallest average grain size of the zinc deposits (38 nm) was obtained at a pulse current density of 1200 mA/cm², as seen from the AFM image (Fig. 5c).

According to several studies [2–5,15], the grain-size refinement observed with increasing pulse current density is attributable to the high overpotential associated with increasing pulse current density. This high overpotential was argued to increase nucleation rate, by increasing the free energy for formation of new nuclei, and therefore refine the grain size. Puippe [15] attained finer grains of gold, copper, palladium, and cadmium electrodeposits at higher pulse current density. Similarly, increasing the pulse current density resulted in a decrease in the grain size of nickel deposits [4]. We [2,3] obtained nanocrystalline zinc, 56 and 50 nm, from a zinc

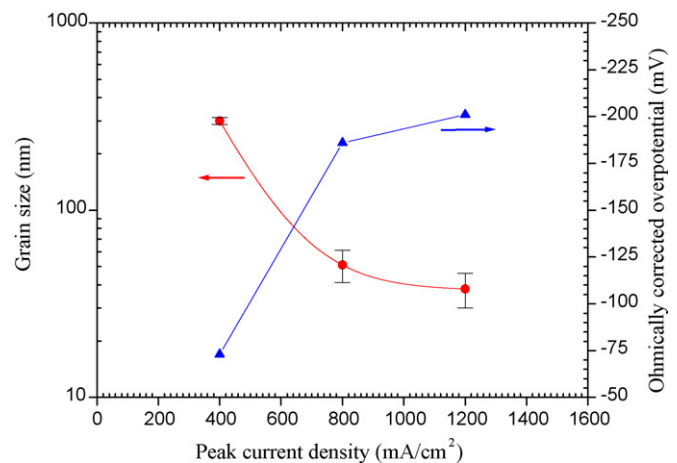


Fig. 6. Variation of grain size and ohmically corrected overpotential of zinc deposits with pulse current density at $T_{\text{on}} = 7$ ms, and $T_{\text{off}} = 9$ ms.

chloride-based electrolyte with additives at high pulse current densities, 2000 and 1000 mA/cm², respectively, and different combinations of current on- and off-times. The above explanations are in good agreement with our results in this study too. The formation of the smallest nanocrystalline zinc deposits (38 nm) is obtained at the highest pulse current density (1200 mA/cm²), which provides the highest cathodic overpotential (–201 mV) obtained under the studied ranges of pulse plating parameters (T_{on} , T_{off} , and J_p) (Fig. 6).

3.4. A hypothesis about evolution of the preferred orientation

Fig. 7 shows the percentage of crystallographic planes of the zinc deposit as a function of angles from the basal plane (0002) at current on-times of 1, 3, 5, and 7 ms with a constant current off-time of 9 ms and pulse current density of 800 mA/cm². These graphs rep-

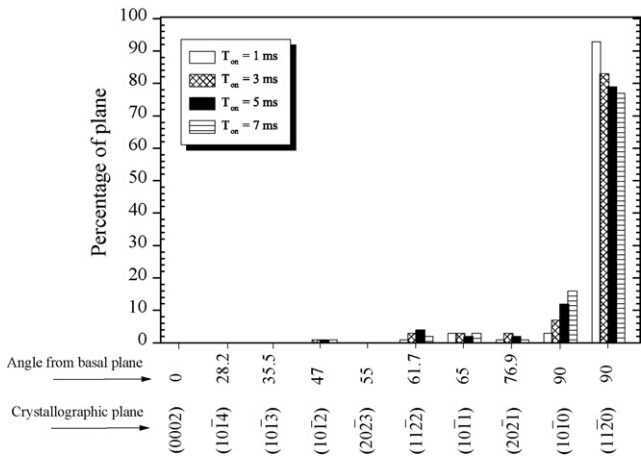


Fig. 7. Schematic representations of percentages of crystallographic planes as a function of angles from basal plane (0002) at $T_{off} = 9$ ms, $J_p = 800$ mA/cm², and various current on-times.

resent a comparison of the relative amount of zinc grains oriented with planes parallel to the substrate. Strong prismatic preferred orientations, (11 $\bar{2}$ 0) and dual (10 $\bar{1}$ 0) (10 $\bar{1}$ 0), were observed with increasing current on-time. A total of 93% of the zinc grains were oriented along the prismatic (11 $\bar{2}$ 0) plane at a current on-time of 1 ms (Fig. 7). Increasing the on-time to 3 ms reduces the tendency of zinc grains to orient along (11 $\bar{2}$ 0) to 83% while the majority of the remaining grains preferred to form another prismatic (10 $\bar{1}$ 0) plane (Fig. 7). Further increase of the current on-time to 5 and 7 ms gradually reduces the percentage of (11 $\bar{2}$ 0) to 79 and 77% and increases that of (10 $\bar{1}$ 0) to 12 and 16%, respectively (Fig. 7).

The crystallographic orientation data of zinc deposits with increasing current off-time is shown in Fig. 8. A sequential reduction in the percentage of the prismatic planes (11 $\bar{2}$ 0) and (10 $\bar{1}$ 0) was realized with increasing current off-time from 9 through 50 ms. It may be noted that high-angle pyramidal (10 $\bar{1}$ 1) and (11 $\bar{2}$ 2) planes and the basal (0002) plane also evolved with increasing current off-time (Fig. 8).

Pulse current density, which has a considerable effect on overpotential, was found to influence the preferred orientation of the zinc deposits. Fig. 9 shows the percentage of crystallographic planes of the zinc deposit as a function of angle from the basal plane (0002). The data were obtained by keeping current on- and off-times constant at 7 and 9 ms, respectively and changing the pulse current density from 400 to 1200 mA/cm². The smallest percentage (54%) of the prismatic (11 $\bar{2}$ 0) plane was obtained at a pulse current density of 400 mA/cm²; however, at the expense of a reduction in the (11 $\bar{2}$ 0) percentage, the high-angle pyramidal (10 $\bar{1}$ 1), (11 $\bar{2}$ 2), and (10 $\bar{1}$ 2) and basal (0002) planes were developed (Fig. 9). Further increase of the pulse current density gradually increases the percentage of the prismatic planes, (11 $\bar{2}$ 0) and (10 $\bar{1}$ 0), up to 61 and 32%, respectively, at 1200 mA/cm² (Fig. 9).

Table 3

Comparison of theoretical and experimental results of preferred orientations for zinc [10], nanocrystalline zinc (present study), and nanocrystalline zinc [3] at low, intermediate, and high overpotentials

Metal	Overpotential					
	Low		Intermediate		High	
	Theoretical	Experimental	Theoretical	Experimental	Theoretical	Experimental
Zinc [10]	(0001)(10 $\bar{1}$ 1)	(0001)(10 $\bar{1}$ 1)	(11 $\bar{2}$ 0)	(11 $\bar{2}$ 0)	(10 $\bar{1}$ 0)(11 $\bar{2}$ 2)	(10 $\bar{1}$ 0)(11 $\bar{2}$ 2)
Zinc (present study)		(10 $\bar{1}$ 1)(11 $\bar{2}$ 0)		(11 $\bar{2}$ 0)		(11 $\bar{2}$ 0)(10 $\bar{1}$ 0)
Zinc [3]		(10 $\bar{1}$ 3)		(11 $\bar{2}$ 0)		(11 $\bar{2}$ 0)(11 $\bar{2}$ 2)

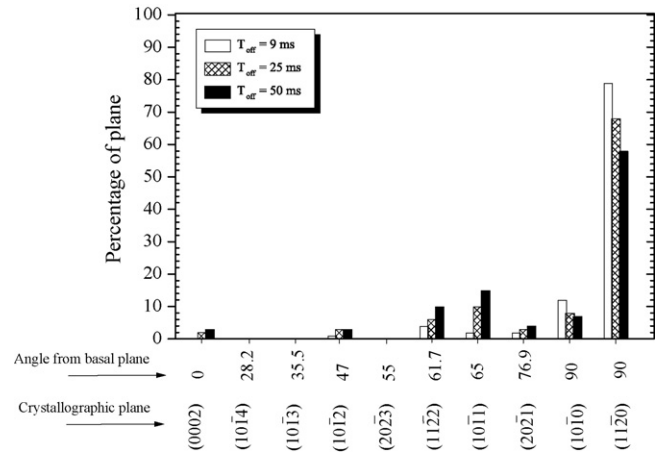


Fig. 8. Schematic representations of percentages of crystallographic planes as a function of angles from basal plane (0002) at $T_{on} = 7$ ms, $J_p = 800$ mA/cm², and various current off-times.

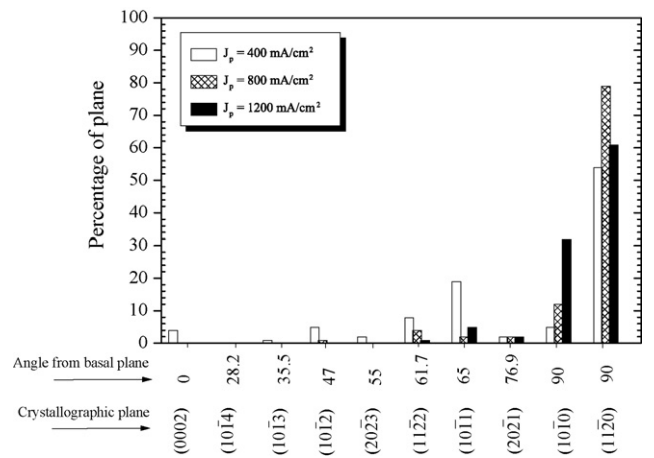


Fig. 9. Schematic representations of percentages of crystallographic planes as a function of angles from basal plane (0002) at $T_{on} = 7$ ms, $T_{off} = 9$ ms, and various pulse current densities.

Preferred orientation develops in electrodeposits because a particular crystal plane(s) is preferentially aligned to the substrate surface [16]. A number of researchers have tried to explain the phenomenon responsible for preferential growth [9,10]. However, most explanations are correlated to either the system being studied and/or a specific material property (e.g., magnetic). One widely accepted hypothesis was developed by Pangarov [10] and is based on two-dimensional nucleation theory. Pangarov calculated the work of formation of two-dimensional nuclei as a function of overvoltage for fcc, bcc, and hcp lattice planes and used these calculations as a basis for a qualitative explanation of preferred orientation as a function of overpotential. Table 3 compares Pan-

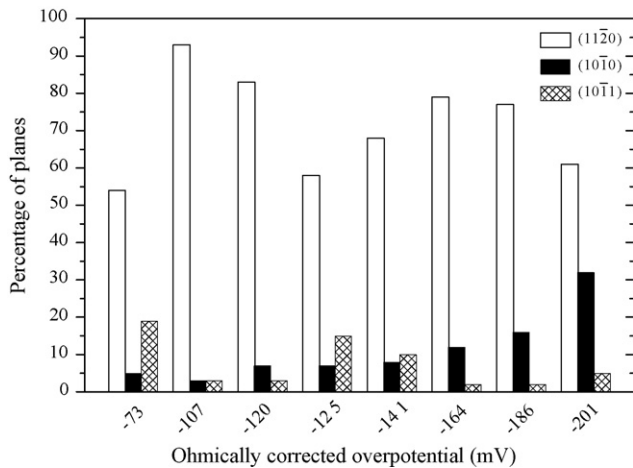


Fig. 10. Variation of crystallographic planes developed during pulse electrodeposition of zinc as a function of overpotential.

garov's results for zinc deposits with our zinc deposits as a function of overpotential (Fig. 10) and also zinc data from reference [3]. It can be seen from Table 3 and Fig. 10 that the most prevalent orientation is that of the $(11\bar{2}0)$ prism plane parallel to the substrate. However, at relatively low overpotential (-73 mV), a dual texture of $(11\bar{2}0)(10\bar{1}1)$ is developed which changed to $(11\bar{2}0)(10\bar{1}0)$ at higher overpotentials. To some extent, our results agree with Pangarov's hypothesis (Table 3). However, the preferred orientations evolved in this study cannot be explained solely based on overpotential and two-dimensional nucleation theory. Other factors, such as the angle between the preferred oriented plane and the lowest energy of formation plane (0002) , might affect the preferred orientation. Fig. 11 shows the expected preferred orientations of zinc deposits as a function of the overpotential and the angle from the lowest energy of formation plane (0002) . It has been postulated [10,13] that conditions corresponding to small overpotential lead to crystallographic orientations of planes hav-

ing high-atomic packing, and preferred orientations of planes that exhibit low-atomic packing requires high cathodic overpotential, i.e., high energy of formation. However, we found a contradiction that $(10\bar{1}0)$, which has a higher packing density than that of $(10\bar{1}1)$ [17], was formed at the highest overpotential (Fig. 9). According to our results, this contradiction might be explained as follows. In principle, pulse electrodeposition is a non-equilibrium process that drives the electrode potential away (more negative) from equilibrium and is therefore capable of producing non-equilibrium structure (nanocrystals) and preferred orientations. If we consider (0002) (closest-packed plane) as the plane that would be developed at a potential near equilibrium (low overpotential), increasing the overpotential (non-equilibrium) would develop planes making certain angles with the equilibrium (0002) plane. The gradual increase of overpotential would gradually increase these angles up to the highest possible value (90°), which corresponds to the prismatic planes $(11\bar{2}0)$ and/or $(10\bar{1}0)$. According to Figs. 7 and 10, about 93% of zinc grains oriented on the prismatic $(11\bar{2}0)$ plane at an overpotential of -107 mV. Decreasing (more positive) the overpotential below -107 mV reduces the percentage of the prismatic $(11\bar{2}0)$ plane and allows some zinc grains to orient on $(10\bar{1}1)$ plane which exhibits the (1) closest high angle (65° with (0002)) and (2) nearest close packed plane to prismatic $(11\bar{2}0)$ (see Fig. 11). However, increasing the cathodic overpotential beyond -107 mV up to -201 mV results in the development of another prismatic (90° with (0002)) plane ($(10\bar{1}0)$) at the expense of $(11\bar{2}0)$ (Figs. 9–11). This result can be explained by the high overpotential that leads to form a $(10\bar{1}0)$ plane, which has a higher energy of formation (lower packing density) than that of $(11\bar{2}0)$ plane.

Not only do the overpotential, the angle between the preferred oriented plane and the lowest energy of formation plane (0002) , and free energy of formation influence the development of preferred orientation, but the pulse plating parameters as well. The reappearance of $(10\bar{1}1)$ plane at overpotentials of -125 and -141 mV can be attributed to the effect of the current off-time. The preferred orientation formed at overpotentials of -125 and -141 mV (Fig. 10) represents the zinc samples deposited at cur-

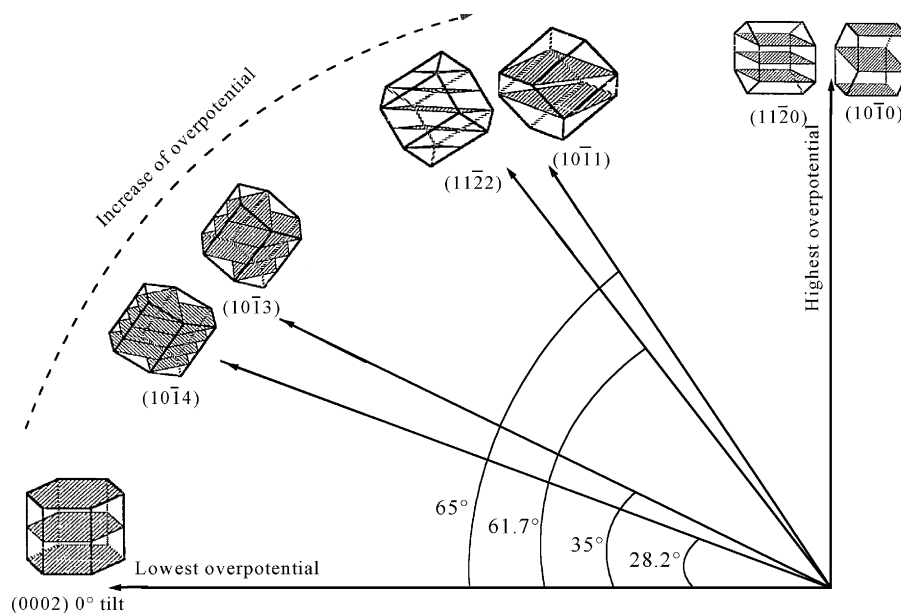


Fig. 11. A schematic representation of the preferred orientations developed in zinc deposits as a function of overpotential and the angle between the preferred oriented plane and the lowest energy of formation plane (0002) .

rent off-times of 50 and 25 ms, respectively (Fig. 8). Zinc adatoms at longer off-times have sufficient time to migrate over the crystal surface and grow on a plane ($(10\bar{1}1)$) having a lower energy of formation than that of the prismatic ($(11\bar{2}0)$).

4. Conclusions

It was found that current on-time, current off-time, and pulse current density have a strong effect on the resulting microstructure and preferred orientation of zinc deposited from a sulfate-based electrolyte. Increasing current on-time in the range of 1–7 ms resulted in grain refinement which was attributed to increased overpotential. Nanocrystalline zinc deposits with an average grain size of 51 nm were produced at current on-time of 7 ms. Increasing the current off-time in the range of 9–50 ms was found to yield grain growth, which was explained by both the decrease of overpotential and longer time for zinc adatoms to surface migrate and enhance the crystal grain-growth process. Grain refinement was also observed by increasing pulse current density, as expected, and a 38 nm average zinc grain size was obtained at a pulse current density of 1200 mA/cm². In terms of preferred orientation, it was found that not only is the overpotential responsible for the textures evolved but also the energy of formation of the crystallographic planes, the angle between the preferred oriented plane and the lowest energy of formation plane (0002), and the pulse plating parameters. Starting from the basal plane (0002), developed at low overpotential, the sequential formation of crystallographic planes with increasing the overpotential depends on the crystallographic angles between these planes and the basal (0002), which has the lowest energy of formation (i.e., equilibrium). The low-angle pyramidal ($10\bar{1}3$) and high-angle pyramidal ($10\bar{1}1$) planes were developed with increasing overpotential. Further increase of the overpotential (i.e., further displacement from equilibrium)

increases the angle up to the highest possible value (90°), which corresponds to the prismatic planes ($(11\bar{2}0)$) and/or ($(10\bar{1}0)$). Furthermore, longer current off-times gives zinc adatoms sufficient time to migrate over the crystal surface and grow on ($10\bar{1}1$) plane that exhibit a lower energy of formation than that of the prismatic ($(11\bar{2}0)$).

Acknowledgments

This work was supported by the International Lead Zinc Research Organization (ILZRO), Dr. Frank E. Goodwin, program manager.

References

- [1] H. Gleiter, *Prog. Mater. Sci.* 33 (1989) 223.
- [2] K.M. Youssef, C.C. Koch, P.S. Fedkiw, *Mater. Sci. Eng. A* 341 (2003) 174.
- [3] K.M. Youssef, P.S. Fedkiw, C.C. Koch, *J. Electrochem. Soc.* 151 (2004) C103.
- [4] A.M. El-Sherik, U. Erb, J. Page, *Surf. Coat. Technol.* 88 (1996) 70.
- [5] M.C. Li, L.L. Jiang, W.Q. Zhang, Y.H. Qian, S.Z. Luo, J.N. Shen, *J. Solid State Electrochem.* 11 (2007) 549.
- [6] A.M. El-Sherik, U. Erb, *J. Mater. Sci.* 30 (1995) 5743.
- [7] J.Cl. Puiippe, N. Ibl, *Plat. Surf. Finish.* 67 (1980) 68.
- [8] W. Paatsch, in: J.Cl. Puiippe, F. Leaman (Eds.), *Theory and Practice of Pulse Plating*, AESF, Orlando, FL, 1986, p. 93.
- [9] A.K. Reddy, *J. Electroanal. Chem.* 6 (1963) 141.
- [10] N.A. Pangarov, *Electrochim. Acta* 7 (1962) 139.
- [11] D.J. Mackinnon, J.M. Brannen, V.I. Lakshmanan, *J. Appl. Electrochem.* 9 (1979) 603.
- [12] L.Ph. Berube, G.L. Esperance, *J. Electrochem. Soc.* 136 (1989) 2314.
- [13] D.I. Rehrig, H. Leidheiser Jr., M.R. Notis, *Plat. Surf. Finish.* 64 (1977) 40.
- [14] S. Yoshimura, S. Chida, E. Sato, *Metal Finish.* 84 (1986) 39.
- [15] J.Cl. Puiippe, in: J.Cl. Puiippe, F. Leaman (Eds.), *Theory and Practice of Pulse Plating*, AESF, Orlando, FL, 1986, p. 17.
- [16] C.S. Barrett, T.B. Massalski, *Structure of Metals*, 3rd edition, McGraw-Hill, Inc., New York, 1966.
- [17] R.W.K. Honeycombe, *The Plastic Deformation of Metals*, 2nd edition, Edward Arnold, Ltd., London, 1984.